University of South Carolina
Scholar Commons

Faculty Publications | Chemical Engineering, Department of

1983

A Model of the Bromine/Bromide Electrode Reaction at a Rotating Disk Electrode

Ralph E. White
University of South Carolina - Columbia, white@cec.sc.edu

S. E. Lorimer
Texas A & M University - College Station

Follow this and additional works at: https://scholarcommons.sc.edu/eche_facpub

 Part of the Chemical Engineering Commons

Publication Info

Journal of the Electrochemical Society, 1983, pages 1096-1103.

This Article is brought to you by the Chemical Engineering, Department of at Scholar Commons. It has been accepted for inclusion in Faculty Publications by an authorized administrator of Scholar Commons. For more information, please contact digres@mailbox.sc.edu.

chem., 6, 353 (1976).
9. S. Meibuhr, E. Yeager, A. Kozawa, and F. Hovorka, *This Journal*, **110**, 190 (1963).
10. V. V. Gorodetskii, I. P. Slutskii, and V. V. Losev, *Elektrokhimiya*, **8**, 1401 (1972).
11. I. P. Slutskii, V. V. Gorodetskii, and V. V. Losev, *ibid.*, **13**, 205 (1977).
12. S. H. Glarum and J. H. Marshall, *This Journal*, **128**, 968 (1981).
13. J. E. B. Randles, *Discuss. Faraday Soc.*, **1**, 11 (1947).
14. C. Deslouis, I. Epelboin, M. Keddam, and J. C. Lestrade, *J. Electroanal. Chem. Interfacial Electrochem.*, **28**, 57 (1970).
15. D. A. Scherson and J. Newman, *This Journal*, **127**, 110 (1980).
16. K. Tokuda and H. Matsuda, *J. Electroanal. Chem. Interfacial Electrochem.*, **82**, 157 (1977); **90**, 149 (1978); **95**, 147 (1979).
17. R. D. Armstrong, M. F. Bell, and A. A. Metcalfe, "Electrochemistry—Spec. Period, Rpts.," Vol. 6, The Chemical Society, London (1978).
18. P. A. Kohl, *This Journal*, **129**, 1196 (1982).
19. A. Vincente and S. Bruckenstein, *Anal. Chem.*, **44**, 297 (1972).
20. H. P. Agarwal and S. Qureshi, *Electrochim. Acta*, **21**, 465 (1976).
21. C. A. Wamser, *J. Am. Chem. Soc.*, **70**, 1209 (1948).
22. A. M. Bond and R. J. Taylor, *J. Electroanal. Chem. Interfacial Electrochem.*, **28**, 207 (1970).
23. M. Pourbaix, "Atlas of Electrochemical Equilibria," Pergamon, London (1966).
24. R. de Levie, *Electrochim. Acta*, **10**, 113 (1965).
25. M. Fleischmann and J. A. Harrison, *ibid.*, **11**, 749 (1966).
26. H. Gerischer, *Z. Phys. Chem.*, **198**, 286 (1951).
27. J. A. Harrison and D. R. Sandbach, *J. Electroanal. Chem. Interfacial Electrochem.*, **85**, 125 (1977).
28. T. D. Hoar, *Trans. Faraday Soc.*, **33**, 1152 (1937).

A Model of the Bromine/Bromide Electrode Reaction at a Rotating Disk Electrode

R. E. White* and S. E. Lorimer*

Department of Chemical Engineering, Texas A&M University, College Station, Texas 77843

ABSTRACT

A mathematical model is presented for the Br_2/Br^- electrode reaction at a rotating disk electrode. The model includes current density-overpotential expressions for the electrode reaction according to either the Volmer-Heyrovsky (V-H) or the Volmer-Tafel (V-T) mechanism and the transport equations including the effect of ionic migration. The model is used to predict current-overpotential curves for various cases of interest. Qualitative comparison of the model predictions to literature data shows that either the V-H or the V-T mechanism, with V controlling, may be acceptable for the Br_2/Br^- reaction.

Table I presents a summary of the investigations of the kinetics of the Br_2/Br^- electrode reaction. The three mechanisms that have been proposed frequently are the Volmer-Heyrovsky (V-H), Volmer-Tafel (V-T), and the Heyrovsky-Tafel (H-T), which can be written as follows

V-H mechanism

$$(V) \quad Br^- \rightleftarrows Br_{ads} + e^- \qquad [1]$$

$$(H) \quad Br_{ads} + Br^- \rightleftarrows Br_2 + e^- \qquad [2]$$

V-T mechanism

$$(V) \quad 2(Br^- \rightleftarrows Br_{ads} + e^-) \qquad [3]$$

$$(T) \quad 2Br_{ads} \rightleftarrows Br_2 \qquad [4]$$

H-T mechanism

$$(H) \quad 2(Br_2 + e^- \rightleftarrows Br^- + Br_{ads}) \qquad [5]$$

$$(T) \quad 2Br_{ads} \rightleftarrows Br_2 \qquad [6]$$

Table I includes the kinetic mechanism(s) proposed by each group, the type of electrode material, and the technique used to determine the kinetics. Also included in the table are comments concerning each group's approach to handling the tribromide ion formation reaction

$$Br_2 + Br^- \underset{k_b}{\overset{k_f}{\leftrightarrows}} Br_3^- \qquad K_{eq} = \frac{k_f}{k_b} \qquad [7]$$

and assumptions made concerning the degree of coverage of the electrode surface with adsorbed bromine (θ) or the rate of adsorption-desorption processes.

Essentially, four different methods have been used to study the kinetics of the Br_2/Br^- electrode reaction. The four methods are: galvanostatic or potentiostatic, impedance, preexponential factor, and coulostatic. Three groups (1, 2, and 3, see Table I) used current density-potential curves produced either galvanostatically or potentiostatically to study the Br_2/Br^- reaction. The kinetic mechanism was selected by comparing the experimentally determined slopes of Tafel curves and reaction orders to those values predicted for each possible electrode kinetic mechanism. Three other groups (4, 5, and 6) measured the impedance of the electrode as a function of the frequency of an applied alternating current and used this to determine the exchange current density. They then determined the dependence of the exchange current density on concentration and overpotential to select the electrode kinetic mechanism. Allard and Parsons (7) used experimentally determined values of the preexponential factor to study Br_2/Br^- electrode kinetics. The order of magnitude of the experimental value of the preexponential factor, which can be determined from measurements of the exchange current density at

Table IA. Summary of Br_2/Br^- kinetic studies

Investigator(s)	Technique	Electrode
1. Osipov *et al.* (1)	Potentiostatic	Platinum RDE
2. Janssen and Hoogland (2)	Galvanostatic	Graphite Stationary
3. Faita, Fiori, and Mussini (3)	Potentiostatic	Platinized Ti RDE
4. Llopis and Vazquez (4)	Impedance	Platinum Stationary
5. Cooper and Parsons (5)	Impedance	Platinum RDE
6. Albery *et al.* (6)	Impedance	Platinum RRDE
7. Allard and Parsons (7)	Preexponential	Platinum RDE
8. Rubinstein (8)	Coulostatic	Platinum Stationary

* Electrochemical Society Active Member.
Key words: battery, migration.

Downloaded 09 Jun 2011 to 129.252.106.20. Redistribution subject to ECS license or copyright; see http://www.ecsdl.org/terms_use.jsp

Table IB. Summary of Br_2/Br^- kinetic studies

Investigator(s)	Proposed mechanism	Rate-controlling step	Comments
1	V-H	Both equally	Ignored tribromide ion formation and adsorption effects
2	V-H	V	Ignored tribromide ion formation; included surface coverage
3	V-H	Both equally	Low surface coverage assumed; ignored tribromide ion formation
4	Slightly modified H-T	H	Ignored tribromide ion formation; experimental data indicated adsorption did not effect electrode reaction rate
5	V-H or V-T (Low surface coverage)	V	Ignored tribromide ion formation
	V-T or H-T (High surface coverage)	T	
6	V-H or V-T	V	Reaction thought to occur in sparsely filled second layer on top of an electrode surface completely covered with a layer of unreactive bromine atoms.
7	V-T	V	Corrections made for tribromide ion formation; estimate made of the degree of surface coverage
8	V-T or V-H (Oxidized electrodes)	V	Used a combined isotherm approach to account for adsorption
	Slightly modified V-T or V-H (Reduced electrodes)	V	

different temperatures, was then used to identify the rate-determining step of various mechanisms. Rubinstein (8) used the coulostatic method which consists of charge injection followed by an open-circuit transient analysis to obtain the kinetic parameters. As before, these parameters are then compared to those predicted by the proposed mechanisms to determine acceptable mechanisms.

As can be seen from Table I, no single electrode kinetic mechanism is supported by all of the investigators. The V-H and V-T mechanisms are, however, suggested more often than the H-T mechanism. Table I also shows that most workers neglected the formation of tribromide ion. This is unfortunate because at the very least this causes confusion concerning the bulk concentrations of the reacting species (Br_2 and Br^-). Finally, Table I entries and other studies reveal that considerable confusion exists over the role of adsorbed bromine in the electrode reaction. Equilibrium values for the degree of coverage of platinum surfaces with adsorbed bromine indicate that as many as 55-60% of the available adsorption sites are covered (9, 10). Also, bromine is known to be strongly chemisorbed on platinum (11-13). On the other hand, the values of the preexponential factor for the bromine electrochemical reaction measured by Allard and Parsons (7) indicate that the degree of surface coverage is low and that the adsorbed species has a high degree of mobility across the electrode surface. Also, the impedance measurements made by Llopis and Vazquez (4) indicated that the rate of the bromine/bromide reaction is not affected by adsorption. To explain these apparently conflicting results, Allard and Parsons (7) proposed that the electrode reaction involves a loosely adsorbed reactive bromine species existing in a sparsely filled layer on top of a layer of unreactive bromine adsorbed directly on the electrode surface. Albery *et al.* (6) and Rubinstein (8) support this proposal.

It is clear that there is still uncertainty concerning the Br_2/Br^- electrode reaction. The kinetic mechanism and associated issues such as the effect of the homogeneous tribromide formation reaction and the role of adsorption-desorption processes in the electrode reaction are still unresolved.

A model is presented here which may be useful for analysis of potentiostatic RDE data. The model includes rate expressions for either the V-H or the V-T mechanisms and is used here to predict current-potential curves for both mechanisms for various cases of interest.

Model

Figure 1 presents a schematic of the RDE system in which the position of the reference electrode is shown. The model presented here consist of current-overpotential expressions for either the V-H or the V-T mechanisms, the transport equations, and the boundary conditions for the RDE system. The model is presented by first listing the assumptions and then the equations.

Assumptions

1. The rates of the individual steps in each of the reaction mechanisms are equal (*i.e.*, $i_V = i_H$ and $i_V = i_T$). Also, for the V-H mechanism, $i = i_V + i_H$ and for V-T mechanism, $i = i_V = i_T$ (14).
2. The double layer is ignored by assuming that it is infinitely thin.
3. Equilibrium adsorption of the adsorbed bromine (Br_{ads}) follows the Langmuir isotherm and is very small ($\theta_o << 1$).
4. The rates of the adsorption-desorption process are rapid enough to not interfere with the rates of the charge transfer steps.
5. The electrolyte is an ideal solution (*i.e.*, concentrations instead of activities are used).
6. Infinitely dilute solution theory (15) applies.
7. The RDE is an equipotential electrode and is uniformly accessible.
8. Steady-state conditions exist.
9. Isothermal conditions exist.

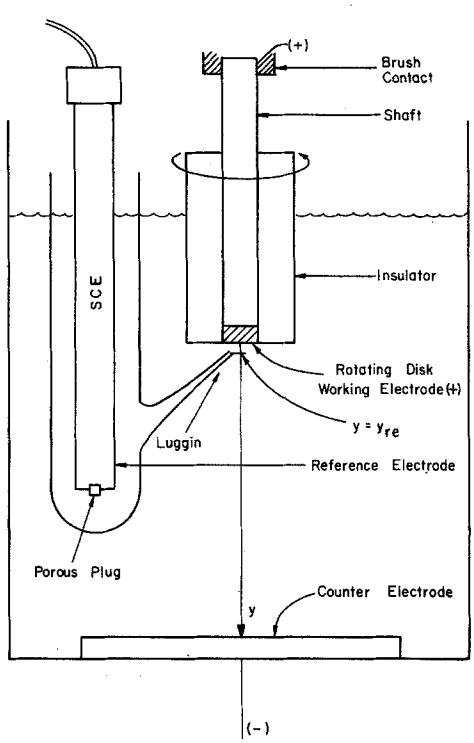

Fig. 1. Schematic of a rotating disk electrode system

Downloaded 09 Jun 2011 to 129.252.106.20. Redistribution subject to ECS license or copyright; see http://www.ecsdl.org/terms_use.jsp

10. The electrolyte is Newtonian and the physical and transport properties are constants.
11. The Nernst-Einstein equation ($u_i = D_i/RT$) is a valid approximation.
12. The reaction orders are given by the stoichiometry of the individual steps of the overall reaction.

Kinetic Equations

The above assumptions and the rate expressions given by Jansson and Hoogland (14) for the Cl_2/Cl^- electrode reaction can be used to derive current density-potential expressions for the V-H and V-T mechanisms, as discussed by Lorimer (16). Essentially the method consists of using assumption 1 to obtain an expression for the current density i for each mechanism which depends on, among other things, the surface coverage and the equilibrium surface coverage of adsorbed bromine atoms. These equations can then be simplified by using assumption 3. The resulting expressions for the V-H and V-T mechanisms are as follows

V-H mechanism

$$i = 2i_{\text{Oref,H}} \exp\left(\frac{(1+\alpha_H)\mathbf{F}}{RT}(\Phi_{\text{met}} - \Phi_o - U_{\text{ref}})\right) \times \frac{\left[\left(\frac{c_{\text{Br}^-,o}}{c_{\text{Br}^-,\text{ref}}}\right)^2 - \left(\frac{c_{\text{Br}_2,o}}{c_{\text{Br}_2,\text{ref}}}\right)\exp\left(\frac{-2\mathbf{F}}{RT}(\Phi_{\text{met}} - \Phi_o - U_{\text{ref}})\right)\right]}{\left[1 + \frac{i_{\text{Oref,H}}}{i_{\text{Oref,V}}}\left(\frac{c_{\text{Br}^-,o}}{c_{\text{Br}^-,\text{ref}}}\right)\exp\left(\frac{(1-\alpha_V+\alpha_H)\mathbf{F}}{RT}(\Phi_{\text{met}} - \Phi_o - U_{\text{ref}})\right)\right]} \quad [8]$$

V-T mechanism

$$i = A + \left[A^2 - \left(i_{\text{Oref,V}}\left(\frac{c_{\text{Br}^-,o}}{c_{\text{Br}^-,\text{ref}}}\right)\exp\left(\frac{\alpha_V\mathbf{F}}{RT}(\Phi_{\text{met}} - \Phi_o - U_{\text{ref}})\right)\right)^2 + \left(i_{\text{Oref,V}}\left(\frac{c_{\text{Br}_2,o}}{c_{\text{Br}_2,\text{ref}}}\right)^{1/2}\exp\left(\frac{-(1-\alpha_V)\mathbf{F}}{RT}\right)(\Phi_{\text{met}} - \Phi_o - U_{\text{ref}})\right)^2\Big]^{1/2} \quad [9]$$

where

$$A = i_{\text{Oref,V}}\left(\frac{c_{\text{Br}^-,o}}{c_{\text{Br}^-,\text{ref}}}\right)\exp\left(\frac{\alpha_V\mathbf{F}}{RT}(\Phi_{\text{met}} - \Phi_o - U_{\text{ref}})\right) + \left(\frac{i_{\text{Oref,V}}}{2i_{\text{Oref,T}}}\right)^2\exp\left(\frac{-2(1-\alpha_V)\mathbf{F}}{RT}(\Phi_{\text{met}} - \Phi_o - U_{\text{ref}})\right) \quad [10]$$

The exchange current densities ($i_{\text{Oref,H}}$, $i_{\text{Oref,V}}$, and $i_{\text{Oref,T}}$) are based on the reference concentrations used in the analysis. These reference exchange current densities are the values that would be obtained from comparison of the predicted and experimental current density-potential curves. Once values for $i_{\text{Oref,j}}$ have been determined they can be adjusted to a standard electrolyte composition by using the following expression

$$i_{\text{Ostd,j}} = i_{\text{Oref,j}} \prod_i \left(\frac{c_{i,\text{std}}}{c_{i,\text{ref}}}\right)^{\gamma_{ij}} \quad [11]$$

where the values of γ_{ij} used here are based on the stoichiometry of the reactions (15, 16) and are presented in Table II. (Even though Br_2 does not participate in the Volmer reaction, Eq. [1], a value for $\gamma_{\text{Br}_2,\text{V}}$, as given in Table II, arises because of the use of assumption 3 in the derivation of Eq. [8] and [9]). The open-circuit potential U_{ref} is based on the reference concentrations and is given by

Table II. Concentration dependence of the exchange current densities

Reaction j	Species i	γ_{ij}
V	Br^-	$1 - \alpha_V$
V	Br_2	$\alpha_V/2$
H	Br^-	$1 - \alpha_H$
H	Br_2	$(1 + \alpha_H)/2$
T	Br^-	0
T	Br_2	1

$$U_{\text{ref}} = U^\theta - U^\theta_{\text{re}} - \frac{RT}{n\mathbf{F}}\sum_i s_i \ln\left(\frac{c_{i,\text{ref}}}{\rho_o}\right) + \frac{RT}{n_{\text{re}}\mathbf{F}}\sum_i s_{i,\text{re}} \ln\left(\frac{c_{i,\text{re}}}{\rho_o}\right) \quad [12]$$

where $c_{i,\text{re}}$ represents the concentration of species i in the reference electrode compartment and both $c_{i,\text{ref}}$ and $c_{i,\text{re}}$ must be in mols/liter in Eq. [12]. This dependence of the open-circuit potential on the reference concentration instead of the surface concentration arises naturally in the derivation of Eq. [8] and [9] due to the concentration dependence of the exchange current density. Also, it should be pointed out that U_{ref} is for the overall reaction ($2Br^- \rightleftarrows Br_2 + 2e^-$).

The above current density-potential expressions can be simplified by assuming that one of the steps is rate controlling or that both steps proceed at approximately the same rate. Table III presents the simplified forms of the rate equations where

$$\eta_{\text{ref}} = \Phi_{\text{met}} - \Phi_o - U_{\text{ref}} \quad [13]$$

Entries IA and IB can be obtained by considering the denominator of Eq. [8]. For $i_{\text{Oref,H}} >> i_{\text{Oref,V}}$ and $|\eta_{\text{ref}}| \leq \sim 0.1$V the term containing the exponential is large relative to one; however, when $|\eta_{\text{ref}}| \geq \sim 0.1$V, the term containing the exponential is small relative to one. The reason for this depends on whether η_{ref} is negative or positive. When η_{ref} is negative and is made to be more and more negative, eventually the exponential becomes so small that the entire term is small relative to one. On the other hand, if η_{ref} is positive and is made more positive, eventually the surface concentration of the bromide ion ($c_{\text{Br}^-,o}$) becomes so small that the entire term is small relative to one, assuming, of course, that the bromide ion is not present in the electrolyte in abundance. The kinetic parameters from these simplified forms are presented for convenience in Table IV and V for cathodic and anodic values of η_{ref}, respectively.

These simplified equations and parameters are presented for completeness and to aid in understanding the system. However, the simplified equations are not necessary for determination of the kinetic rate constants. Again, the kinetic rate constants should be determined by comparison of the experimental data (current density at a set potential difference between the RDE and a reference electrode) to predicted values from the complete expressions.

Transport Equations

The steady state, no homogeneous reaction material balance equation for species i is (15)

Downloaded 09 Jun 2011 to 129.252.106.20. Redistribution subject to ECS license or copyright; see http://www.ecsdl.org/terms_use.jsp

Table III. Simplified forms of the V-H and V-T current density expressions for limiting cases

I. Volmer-Heyrovsky mechanism (Eq. [8])

A. Volmer reaction rate controlling, low η_{ref} ($i_{o_{ref,H}} >> i_{o_{ref,V}}$, $|\eta_{ref}| \leq \sim 0.1V$)

$$i = 2i_{o_{ref,V}}\left[\left(\frac{c_{Br^-,O}}{c_{Br^-,ref}}\right)\exp\left(\frac{\alpha_V F}{RT}\eta_{ref}\right) - \left(\frac{c_{Br_2,O}}{c_{Br_2,ref}}\right)\left(\frac{c_{Br^-,O}}{c_{Br^-,ref}}\right)^{-1}\exp\left(\frac{-(2-\alpha_V)F}{RT}\eta_{ref}\right)\right]$$

B. Volmer reaction rate controlling, high η_{ref} ($i_{o_{ref,H}} >> i_{o_{ref,V}}$, $|\eta_{ref}| \geq \sim 0.1V$)

$$i = 2i_{o_{ref,H}}\left[\left(\frac{c_{Br^-,O}}{c_{Br^-,ref}}\right)^2\exp\left(\frac{(1+\alpha_H)F}{RT}\eta_{ref}\right) - \left(\frac{c_{Br_2,O}}{c_{Br_2,ref}}\right)\exp\left(\frac{-(1-\alpha_H)F}{RT}\eta_{ref}\right)\right]$$

C. Heyrovsky reaction rate controlling ($i_{o_{ref,V}} >> i_{o_{ref,H}}$)

$$i = 2i_{o_{ref,H}}\left[\left(\frac{c_{Br^-,O}}{c_{Br^-,ref}}\right)^2\exp\left(\frac{(1+\alpha_H)F}{RT}\eta_{ref}\right) - \left(\frac{c_{Br_2,O}}{c_{Br_2,ref}}\right)\exp\left(\frac{-(1-\alpha_H)F}{RT}\eta_{ref}\right)\right]$$

D. Both reactions approximately equally rate controlling ($i_{o_{ref,V}} \approx i_{o_{ref,H}}$)

1. Cathodic overpotential (anodic back reaction neglected)

$$i = -2i_{o_{ref,H}}\left(\frac{c_{Br^-,O}}{c_{Br^-,ref}}\right)\exp\left(\frac{(1+\alpha_H)F}{RT}\eta_{ref}\right)$$

2. Anodic overpotential (cathodic back reaction neglected)

$$i = 2i_{o_{ref,V}}\left(\frac{c_{Br^-,O}}{c_{Br,ref}}\right)\exp\left(\frac{\alpha_V F}{RT}\eta_{ref}\right)$$

II. Volmer-Tafel mechanism (Eq. [9] and [10])

A. Volmer reaction rate controlling ($i_{o_{ref,T}} >> i_{o_{ref,V}}$)

$$i = i_{o_{ref,V}}\left[\left(\frac{c_{Br^-,O}}{c_{Br^-,ref}}\right)\exp\left(\frac{\alpha_V F}{RT}\eta_{ref}\right) - \left(\frac{c_{Br_2,O}}{c_{Br_2,ref}}\right)^{1/2}\exp\left(\frac{-(1-\alpha_V)F}{RT}\eta_{ref}\right)\right]$$

B. Tafel reaction rate controlling ($i_{o_{ref,V}} >> i_{o_{ref,T}}$)

$$i = i_{o_{ref,T}}\left[\left(\frac{c_{Br^-,O}}{c_{Br^-,ref}}\right)^2\exp\left(\frac{2F}{RT}\eta_{ref}\right) - \left(\frac{c_{Br_2,O}}{c_{Br_2,ref}}\right)\right]$$

C. Both reactions approximately equally rate controlling ($i_{o_{ref,V}} \approx i_{o_{ref,T}}$)

1. Cathodic overpotentials (anodic back reaction neglected)
No simplified form of the V-T current density expression is available for this case except near limiting current where

$$i = -i_{o_{ref,T}}\left(\frac{c_{Br_2,O}}{c_{Br_2,ref}}\right)$$

2. Anodic overpotentials (cathodic back reaction neglected)

$$i = i_{o_{ref,V}}\left(\frac{c_{Br^-,O}}{c_{Br^-,ref}}\right)\exp\left(\frac{\alpha_V F}{RT}\eta_{ref}\right)$$

$$-\frac{dN_i}{dy} = 0 \qquad [14]$$

where N_i is the flux of species i. The flux of species i occurs by three mass transfer processes: ionic migration, diffusion, and convection and is given by

$$N_i = -z_i\frac{D_i F c_i}{RT}\frac{d\Phi}{dy} - D_i\frac{dc_i}{dy} + v_y c_i \qquad [15]$$

Newman (15), for example, shows that at high Schmidt numbers, the component of fluid velocity in

Table IV. Electrode kinetic parameters from simplified forms of current density expressions for cathodic η_{ref}

Kinetic mechanism	Rate-determining step	2.303 / Tafel slope (in volts)	Tafel line intercept	Reaction orders q_{Br_2}	Reaction orders q_{Br^-}
V-H	Volmer, $-\eta_{ref} \leq \sim 0.1V$	$\frac{(2-\alpha_V)F}{RT}$	$2i_{o_{ref,V}}$	1	−1
	Volmer, $-\eta_{ref} \geq \sim 0.1V$	$\frac{(1-\alpha_H)F}{RT}$	$2i_{o_{ref,H}}$	1	0
	Heyrovsky	$\frac{(1-\alpha_H)F}{RT}$	$2i_{o_{ref,H}}$	1	0
	Approximately equal	$\frac{(1-\alpha_H)F}{RT}$	$2i_{o_{ref,H}}$	1	0
V-T	Volmer	$\frac{(1-\alpha_V)F}{RT}$	$i_{o_{ref,V}}$	½	0
	Tafel	0	$i_{o_{ref,T}}$	1	0
	Approximately equal	0	$i_{o_{ref,T}}$	1	0

Table V. Electrode kinetic parameters from simplified forms of current density expressions for anodic η_{ref}

Kinetic mechanism	Rate determining step	2.303 / Tafel slope (in volts)	Tafel line intercept	Reaction orders p_{Br_2}	Reaction orders p_{Br^-}
V-H	Volmer, $\eta_{ref} \leq \sim 0.1V$	$\frac{\alpha_V F}{RT}$	$2i_{o_{ref,V}}$	0	1
	Volmer, $\eta_{ref} \geq \sim 0.1V$	$\frac{(1+\alpha_H)F}{RT}$	$2i_{o_{ref,H}}$	0	2
	Heyrovsky	$\frac{(1+\alpha_H)F}{RT}$	$2i_{o_{ref,H}}$	0	2
	Approximately equal	$\frac{\alpha_V F}{RT}$	$2i_{o_{ref,V}}$	0	1
V-T	Volmer	$\frac{\alpha_V F}{RT}$	$i_{o_{ref,V}}$	0	1
	Tafel	$\frac{2F}{RT}$	$i_{o_{ref,T}}$	0	2
	Approximately equal	$\frac{\alpha_V F}{RT}$	$i_{o_{ref,V}}$	0	1

Downloaded 09 Jun 2011 to 129.252.106.20. Redistribution subject to ECS license or copyright; see http://www.ecsdl.org/terms_use.jsp

the directional normal to the electrode surface is given by

$$v_y = -a\Omega(\Omega/\nu)^{1/2}y^2 \quad [16]$$

where y is the distance from the electrode into the electrolyte in a direction normal to the electrode surface. This coordinate can be rewritten in dimensionless form as

$$\xi = y\left(\frac{\nu_a}{3D_R}\right)^{1/3}\left(\frac{\Omega}{\nu}\right)^{1/2} \quad [17]$$

or

$$\xi = y/\delta_D \quad [18]$$

where δ_D is the diffusion layer thickness and is given by

$$\delta_D = \left(\frac{3D_R}{\nu_a}\right)^{1/3}\left(\frac{\nu}{\Omega}\right)^{1/2} \quad [19]$$

Substitution of Eq. [15], [16], and [18] into Eq. [14] yields

$$D_i\frac{d^2c_i}{d\xi^2} + 3D_R\xi^2\frac{dc_i}{d\xi} + \frac{z_iD_iF}{RT}\left[c_i\frac{d^2\Phi}{d\xi^2} + \frac{dc_i}{d\xi}\frac{d\Phi}{d\xi}\right] = 0 \quad [20]$$

which is the material balance equation used here for species i. The electroneutrality condition

$$\sum_i z_ic_i = 0 \quad [21]$$

completes the set of i + 1 equations to be solved subject to the boundary conditions to obtain c_i and Φ.

Boundary Conditions in the Bulk Solution

Bulk solution conditions are assumed to exist at $y = y_{re}$ where y_{re} is the normal distance from the RDE to the reference electrode (see Fig. 1). The concentration of species i in the bulk solution is designated as $c_{i,ref}$ and the potential in the bulk solution at $y = y_{re}$ is designated as Φ_{re}.

Thus, the boundary conditions in the bulk solution are:

at $y = y_{re}$

$$c_i = c_{i,ref} \quad [22]$$

$$\Phi = \Phi_{re} = \text{a set value (0.01V, } e.g.\text{)} \quad [23]$$

where $c_{i,ref}$ must satisfy the electroneutrality condition (Eq. [21]).

Boundary Conditions at the Electrode Surface

The boundary conditions at the electrode surface are as follows:

at $y = 0$

$$\frac{s_ii}{nF} = -N_i \quad [24]$$

$$\sum_i z_ic_i = 0 \quad [25]$$

$$\Phi_{met} = \text{a set value (0.1V, } e.g.\text{)} \quad [26]$$

where N_i is given by Eq. [15] with $v_y = 0$ and i is given by either Eq. [8] or [9].

The potentials in the boundary conditions given by Eq. [23] and [26] are shown schematically in Fig. 2 for a rotating disk electrode being operated anodically. Note that the potential difference between the working electrode and the reference electrode ($\Phi_{met} - \Phi_{re}$) is the quantity set by a potentiostat. In the model, however, both Φ_{met} and Φ_{re} are set independently such that their difference is equal to that set by the potentiostat.

Solution Technique

The i + 1 set of governing equations for c_i and Φ (Eq. [20] and [21]) can be solved numerically subject to the boundary conditions (Eq. [22]-[26]) once values have been specified for the following parameters: $c_{i,ref}$, D_i, ρ_o, ν, T, U^θ, s_i, n, type of reference electrode, $s_{i,re}$, $c_{i,re}$, y_{re}, $i_{Oref,j}$, α_V, α_H, (if necessary) Ω, and Φ_{met}, and Φ_{re} (again, only $\Phi_{met} - \Phi_{re}$ is important). Newman's (15) numerical technique [see also White (17)] can be used to solve this set of equations which yields values for the variable quantities Φ_o, $c_{Br^-,o}$, and $c_{Br_2,o}$. These values together with either Eq. [8] or [9] and the values for Φ_{met}, Φ_{re}, and the calculated value U_{ref} yield values for the current density i at a specified value of $\Phi_{met} - \Phi_{re}$ or η_{ref} calculated according to Eq. [13].

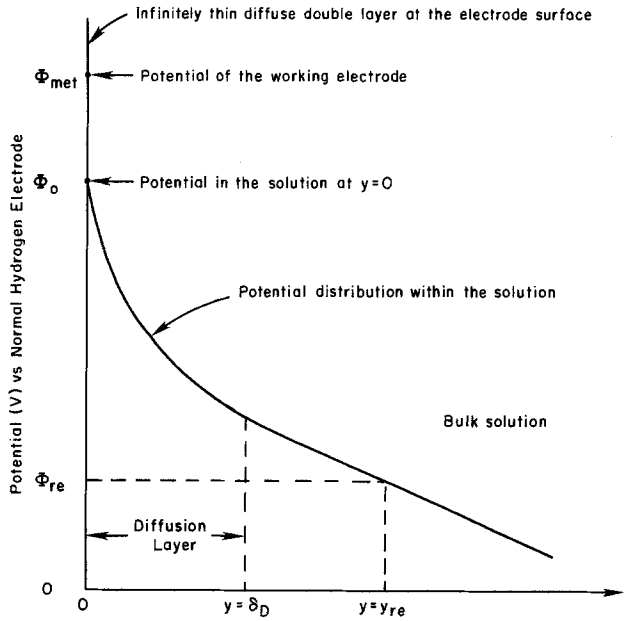

Fig. 2. Schematic of the solution potential profile near an electrode

Results and Discussion

The model presented above can be used to predict the current density for a set potential difference between the working electrode and a reference electrode ($\Phi_{met} - \Phi_{re}$) once the parameter values have been set. Alternatively, the model could be used to determine the kinetic parameters by comparing the predicted current density values to observed values and finding the parameter values that minimize the sum of the squares of the difference between the predicted and measured current densities. However, the model is used here to present predicted current density-potential curves which illustrate some of the capabilities of the model. Also, to simplify the presentation, the tribromide ion formation reaction is neglected completely (additional work which includes the formation of Br_3^- may be presented in the future).

Table VI presents the fixed parameter values used in the model to produce the predicted current-potential curves shown in Fig. 3-7. Figure 3 presents the effect of varying the magnitude of the exchange current densities in the V-H mechanism with $i_{Oref,H}/i_{Oref,V} = 1.0$. As shown in Fig. 3, an order of magnitude change in the exchange current densities yields noticeably different cathodic current-potential curves. Figure 4 shows the effect of the magnitude of the exchange current densities for the V-T mechanism with the Volmer step controlling ($i_{Oref,V}/i_{Oref,T} = 0.01$). Notice that the predicted limiting current densities depend on the magnitude of the exchange current densities even though the Volmer step is rate controlling. Note also that the limiting current density predicted by Levich equation (15)

$$i_{LD} = -0.62Fc_{Br_2,ref}(\Omega\nu)^{1/2}\left(\frac{D_{Br_2}}{\nu}\right)^{2/3}$$

Downloaded 09 Jun 2011 to 129.252.106.20. Redistribution subject to ECS license or copyright; see http://www.ecsdl.org/terms_use.jsp

Table VI. Fixed parameter values

Parameter	Value
Reference concentrations	$c_{K^+,ref} = 2.01 \times 10^{-3}$ mol/cm³ $c_{Br^-,ref} = 1.0 \times 10^{-5}$ mol/cm³ $c_{SO_4^{2-},ref} = 1.0 \times 10^{-3}$ mol/cm³
Diffusion and stoichiometric coefficients	$D_{K^+} = 1.957 \times 10^{-5}$ cm²/sec[a] $s_{K^+} = 0$ $D_{SO_4^{2-}} = 1.065 \times 10^{-5}$ cm²/sec[a] $s_{SO_4^{2-}} = 0$ $D_{Br^-} = 2.084 \times 10^{-5}$ cm²/sec[a] $s_{Br^-} = 2$ $D_{Br_2} = 1.2 \times 10^{-5}$ cm²/sec[b] $s_{Br_2} = -1$
Miscellaneous:	
Pure solvent density (ρ_0)	1.0 g/cm³
Kinematic viscosity (ν)	1.0×10^{-2} cm²/sec
Temperature (T)	298.15 K
Equilibrium electrode potential (U_{ref})	0.904V, for reference concentrations and a saturated calomel reference electrode
Reference electrode position[c] (y_{re})	0.01 cm

[a] Newman (15).
[b] Osipov *et al.* (1).
[c] Picked for convenience.

is not obtained until the values of the exchange current densities are larger than expected. This means that the exchange current density for the Tafel reaction is probably larger than the exchange current density for Volmer reaction by more than two orders of magnitude.

Figure 5 shows the effect of the Heyrovsky transfer coefficient (α_H) in the V-H mechanism for the case where the Heyrovsky step is rate controlling and Fig. 6 shows the effect of α_V when the Volmer step is controlling. Both figures show that transfer coefficients change the shape of the entire curve.

Figure 7 presents the effect of α_V on the predicted current density-potential curves for the V-T mechanism. Notice that the small exchange current density for the Tafel step indicating that it is the rate-controlling step prevents a noticeable change in the curve when α_V is changed from 0.1 to 0.9.

Qualitative comparison of predicted current density-potential curves based on the model presented here to those given by Osipov *et al.* (1) reveals that either the V-H or the V-T mechanism with the Volmer step rate controlling may be an acceptable mechanism for the Br_2/Br^- electrode reaction. Additional raw data are necessary for a complete comparison which may permit a more definitive statement about the Br_2/Br^- mechanism.

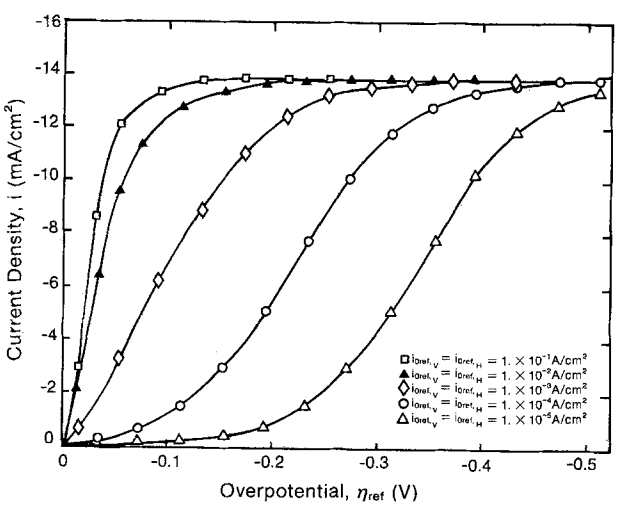

Fig. 3. Effect of the magnitude of the exchange current densities for the V-H mechanism with $i_{Oref,H}/i_{Oref,V} = 1.0$, $\alpha_V = \alpha_H = 0.5$, rotation speed = 1000 rpm.

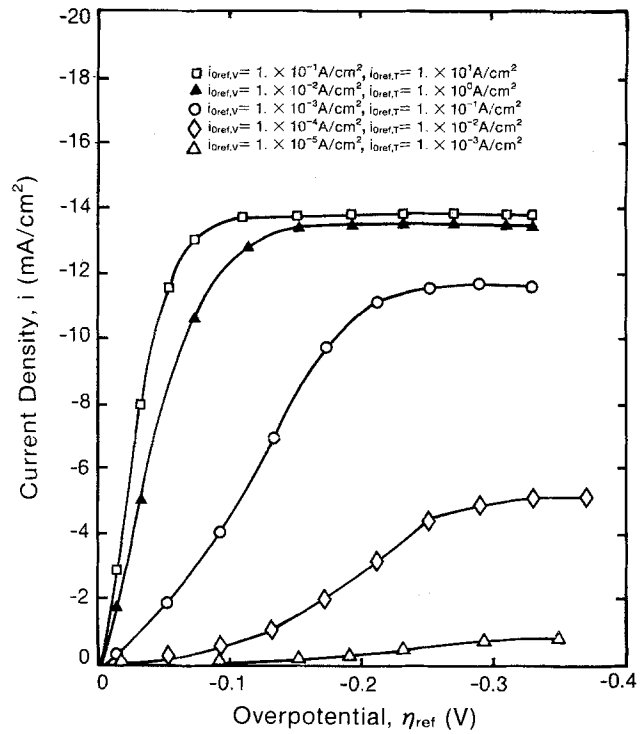

Fig. 4. Effect of a change in the exchange current density magnitude on cathodic current density curves predicted with the model for V-T kinetics. Volmer reaction rate controlling. $\alpha_V = 0.5$, rotation speed = 1000 rpm.

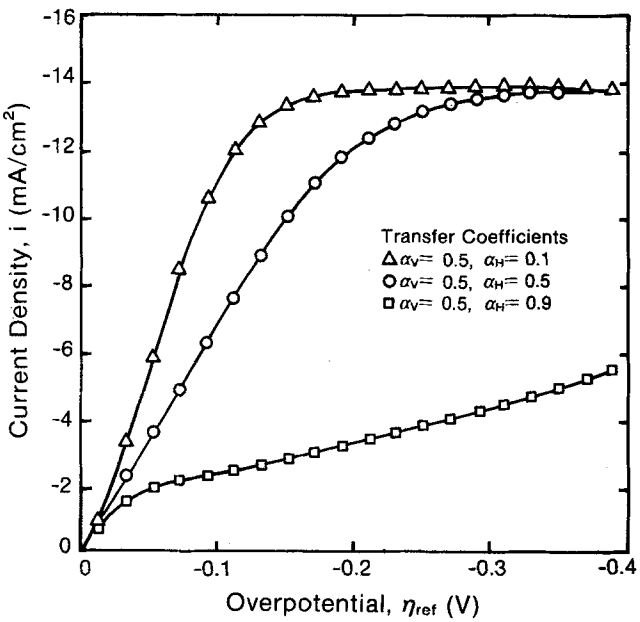

Fig. 5. Effect of a change in Heyrovsky transfer coefficient value on cathodic current density curves predicted with the model for V-H kinetics. Heyrovsky reaction rate controlling. $i_{Oref,V} = 1 \times 10^{-1}$ A/cm², $i_{Oref,H} = 1 \times 10^{-2}$, rotation speed = 1000 rpm.

Conclusion

The current density expressions presented here for the V-H and V-T mechanisms can be used to predict current density-overpotential curves which are similar to data. Qualitative comparison of the predictions of the model presented here to data shows that either the V-H mechanism or the V-T mechanism with the Volmer reaction controlling is an acceptable mechanism for the Br_2/Br^- reaction.

Downloaded 09 Jun 2011 to 129.252.106.20. Redistribution subject to ECS license or copyright; see http://www.ecsdl.org/terms_use.jsp

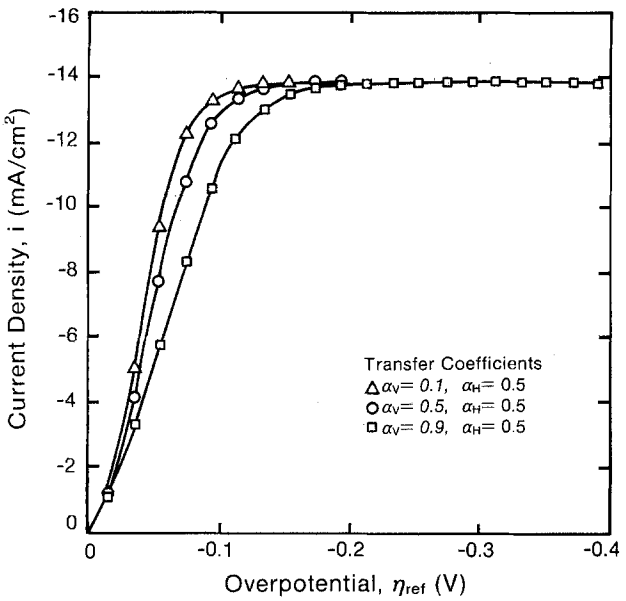

Fig. 6. Effect of a change in Volmer transfer coefficient value on cathodic current density curves predicted with the model for V-H kinetics. Volmer reaction rate controlling. $i_{Oref,V} = 1 \times 10^{-3}$ A/cm², $i_{Oref,H} = 1 \times 10^{-1}$ A/cm², rotation speed = 1000 rpm.

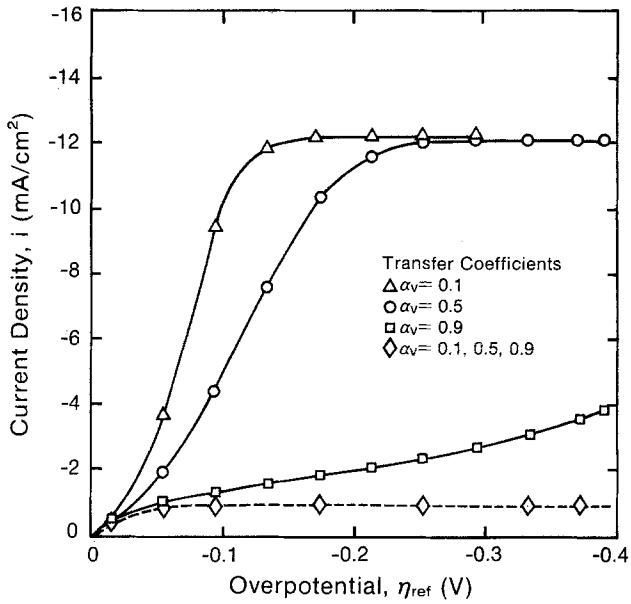

Fig. 7. Effect of a change in Volmer transfer coefficient value on cathodic current density curves predicted with the model for V-T kinetics using two sets of exchange current density values. $i_{Oref,V} = 1 \times 10^{-1}$ A/cm², $i_{Oref,T} = 1 \times 10^{-3}$ A/cm² (- - -); $i_{Oref,V} = 1 \times 10^{-3}$ A/cm², $i_{Oref,T} = 1 \times 10^{-1}$ A/cm² (———).

Acknowledgments

This work was supported by NSF Grant Number ENG-7908071 and by the Center for Energy and Mineral Resources of Texas A&M University.

Manuscript submitted Oct. 14, 1982; revised manuscript received Jan. 3, 1983.

Any discussion of this paper will appear in a Discussion Section to be published in the December 1983 JOURNAL. All discussions for the December 1983 Discussion Section should be submitted by Aug. 1, 1983.

LIST OF SYMBOLS

a	0.51023
$c_{i,std}$	standard concentration of species i (mol/cm³)
$c_i(y)$	concentration of species i at distance y from electrode (mol/cm³)
D_i	diffusion coefficient of species i (cm²/sec)
D_R	diffusion coefficient of limiting reactant (cm²/sec), chosen to be Br_2 here
$\mathbf{F}$	Faraday's constant, 96,487 C/mol
i	current density (A/cm²)
i_{LD}	limiting current density determined by convection and diffusion, value given by Levich equation (A/cm²)
$i_{Ostd,j}$	exchange current density for reaction j at standard concentrations (A/cm²)
$i_{Oref,j}$	exchange current density for reaction j at reference concentrations (A/cm²)
K_{eq}	equilibrium constant for homogeneous tribromide formation reaction (cm³/mol)
k_b	backward reaction rate constant for tribromide homogeneous reaction (sec⁻¹)
k_f	forward reaction rate constant for tribromide homogeneous reaction (cm³/mol-sec)
N_i	flux of species i (mol/cm²-sec)
n	number of electrons transferred in the overall electrode reaction ($n = 2$ here)
p_i	anodic reaction order of species i
q_i	cathodic reaction order of species i
R	universal gas constant, 8.3143 J/mol K
s_i	stoichiometric coefficient for species i in overall electrochemical reaction
T	temperature (K)
U	standard potential of an electrode reaction on hydrogen electrode scale (V)
U^θ_{re}	standard potential of reference electrode reaction on hydrogen electrode scale (V)
U^θ_{ref}	equilibrium potential difference between working electrode and reference electrode evaluated with chosen reference concentrations (V)
u_i	mobility of species i (cm²-mol/J-sec)
v_y	component of velocity of electrolyte flow in a direction normal to the electrode surface (cm/sec)
y	distance from electrode in a direction normal to the electrode surface (cm)
z_i	charge on species i
α_j, $(1 - \alpha_j)$	anodic and cathodic transfer coefficients of reaction j
γ_{ij}	power on concentration term for species i in reaction j in expressions for exchange current densities
δ_D	diffusion layer thickness (cm)
η_{ref}	overpotential expressing departure of electrode reaction driving force ($\Phi_{met} - \Phi_o$) from equilibrium value corresponding to chosen reference concentrations (V)
θ_o	equilibrium surface coverage of adsorbed bromine
ν	kinematic viscosity of the electrolyte (cm²/sec)
ξ	dimensionless distance from electrode surface (y/δ_D)
ρ_o	pure solvent density (g/cm³)
Φ	potential in the solution as sensed by a reference electrode (V)
Φ_{re}	potential in the bulk solution at the reference electrode as sensed by a reference electrode at $y = y_{re}$ (V)
Φ_o	potential in the electrolyte immediately adjacent to working electrode surface as sensed by a reference electrode (V)
Φ_{met}	potential of the working electrode (RDE) with respect to the same thermodynamic potential scale as the reference electrode in the solution (V)
Ω	disk rotational speed (rad/sec)

Subscripts

H	identifies the value of a quantity associated with the Heyrovsky reaction
R	denotes quantity associated with the limiting reactant
re	refers to the reference electrode
ref	identifies a value associated with a chosen set of reference concentrations (*e.g.*, $c_{i,ref}$, $i_{Oref,j}$)
std	identifies a value associated with a chosen set of standard concentrations
T	identifies the value of a quantity associated with the Tafel reaction
V	identifies the value of a quantity associated with the Volmer reaction
o	subscript, denoting a quantity which is evaluated with the concentration adjacent to the electrode surface (except for θ_o and ρ_o)

Downloaded 09 Jun 2011 to 129.252.106.20. Redistribution subject to ECS license or copyright; see http://www.ecsdl.org/terms_use.jsp

REFERENCES

1. O. R. Osipov, M. A. Novitskii, Yu. M. Povarov, and P. D. Lukovtsev, *Elektrokhimiya*, **8**, 327 (1972).
2. L. J. J. Janssen and J. G. Hoogland, *Electrochim. Acta*, **15**, 1677 (1972).
3. G. Faita, G. Fiori, and T. Mussini, *ibid.*, **13**, 1765 (1968).
4. J. Llopis and M. Vasquez, *ibid.*, **6**, 167, 177 (1962).
5. W. D. Cooper and R. Parsons, *Trans. Faraday Soc.*, **66**, 1968 (1970).
6. W. J. Albery, A. H. Davis, and A. J. Mason, *Faraday Discuss. Chem. Soc.*, **56**, 317 (1973).
7. D. Allard and R. Parsons, *Chem.-Ing.-Tech.*, **44**, 201 (1972).
8. I. Rubinstein, *J. Phys. Chem.*, **85**, 13 (1981).
9. V. S. Vilinskaya and M. R. Tarasevich, *Elektrokhimiya*, **7**, 1515 (1971).
10. V. S. Bagotzky, Yu. B. Yassilyev, J. Weber, and J. N. Pirtskhalava, *J. Electroanal. Chem. Interfacial Electrochem.*, **27**, 31 (1970).
11. M. W. Breiter, *Electrochim. Acta*, **8**, 925 (1963).
12. N. A. Balashova and K. E. Kazarinov, *Electroanal. Chem.*, **3**, 135 (1969).
13. R. F. Lane and A. T. Hubbard, *J. Phys. Chem.*, **79**, 808 (1975).
14. L. J. J. Janssen and J. G. Hoogland, *Electrochim. Acta*, **15**, 941 (1972).
15. J. S. Newman, "Electrochemical Systems," Prentice-Hall, Englewood Cliffs, NJ (1973).
16. S. E. Lorimer, M.S. Thesis, Texas A&M University, College Station, TX (1982).
17. R. E. White, *Ind. Eng. Chem. Fundam.*, **17**, 367 (1978).

Technical Notes

A Technique for Calculating Shunt Leakage and Cell Currents in Bipolar Stacks Having Divided or Undivided Cells

E. A. Kaminski and R. F. Savinell*

Department of Chemical Engineering, The University of Akron, Akron, Ohio 44325

The design of high-output voltage electrochemical batteries calls for series electrical connection of separate cells. Likewise, in scaling up electrosynthesis processes, simplicity of construction may warrant the building of reactors containing several cells arranged in series. A convenient design for supplying reactants to a cell assembly is to parallel feed the cells with electrolyte distributed by an inlet manifold and collected by an outlet manifold. The electrolyte-filled piping furnishes secondary series electrical connections among the cells. Consequently, the ionic currents generated by electrode processes are driven by the intercell potential gradients of the assembly through conductive paths in the piping. These ionic shunt or bypass currents short-circuit each cell in the assembly causing power loss, corrosion, current inefficiency, and nonuniform cell-to-cell current distribution. The magnitude of the bypass current in an assembly is a function of the number of cells in the assembly, cell voltage (which includes current dependent polarizations), conductivity of the electrolyte, and the geometry of the electrolyte feed system. Thus, bypass current is a parameter in the design of assemblies.

Analysis of bypass current proceeds by applying Kirchhoff's laws to electrical circuit analogs of assemblies. The analog circuits are devised to represent current flow paths by standard electrical components. Most investigators (1) model assemblies by linear, passive, d-c networks, the work of Katz (2) and Onishchuk (3) being exceptions. Katz incorporates into the analog imaginary Zener diodes with different polarization characteristics in the forward and backward current direction. The diodes account for the polarizations of the anodic and cathodic reactions which occur at the ends of the shunt paths. Onishchuk (3) models a cell by a voltage source in series with a nonlinear current dependent resistive element.

Analysis of the analog results in a large set of simultaneous linear or nonlinear equations. Two methods have usually been employed in obtaining solutions. One is simultaneous solution of the governing equations (1, 2, 4, 5). The other is approximating the system of equations by a single differential equation (3, 6). The continuous approximations apply to assemblies with a sufficiently large number of cells.

This study presents a treatment of bypass current based on the solution of finite difference equations. The formalism is applied to assemblies of divided and undivided cells. The analysis yields a set of compact equations for determining branch currents in the circuit analog. Implementation of this computational procedure requires a minimum of programming effort and computer storage as simultaneous solution of equations is avoided. The same equations can be used to simulate an assembly of cells operating as energy or substance producers.

Theory

Circuit analogs are constructed making the usual assumptions (2, 4, 5, 6). Surfaces of the electrolyte distribution system are nonconducting. The electrolyte flow paths are conducting and are represented by resistor elements. All resistance paths between the cells and a manifold are identical, and each manifold segment between a pair of branches is represented by an identical resistor. Cells of assemblies are assumed to have a linear polarization characteristic, while each cell is represented as an ideal voltage source in series with this resistor. Electrodes offer no resistance to current flow. The electrolyte in a cell compartment is assumed to be at a uniform potential throughout.

An analog circuit of an N cell assembly of two-compartment cells which incorporates these assumptions

* Electrochemical Society Active Member.
Key words: shunt currents, bipolar cell, separated cells, current distribution.

Downloaded 09 Jun 2011 to 129.252.106.20. Redistribution subject to ECS license or copyright; see http://www.ecsdl.org/terms_use.jsp